Production of light hypernuclei in Au+Au collisions at $\sqrt{s_{NN}} = 3$ GeV within a thermodynamic approach

M. Kozhevnikova [1,*] and Yu. B. Ivanov [2,3,†]

[1] *Veksler and Baldin Laboratory of High Energy Physics, JINR Dubna, 141980 Dubna, Russia*

[2] *Bogoliubov Laboratory of Theoretical Physics, JINR Dubna, 141980 Dubna, Russia*

[3] *National Research Center "Kurchatov Institute", 123182 Moscow, Russia*

(Received 12 January 2024; accepted 14 February 2024; published 4 March 2024)

Simulations of the Λ-hyperon and light-hypernuclei production in Au+Au collisions at $\sqrt{s_{NN}} = 3$ GeV were performed within the updated three-fluid hydrodynamics-based event simulator extended by UrQMD (ultrarelativistic quantum molecular dynamics) final state interactions (THESEUS). The light (hyper)nuclei are treated thermodynamically, i.e., they are considered on an equal basis with hadrons. The only additional parameter is related to the late freeze-out that imitates the afterburner stage for the light (hyper)nuclei because UrQMD is not able to dynamically treat them. The calculation of hypernuclei production is the same as that of light nuclei. The hypernuclei results are compared with recent STAR data. It is found that the calculated midrapidity ${}^3_\Lambda\mathrm{H}/\Lambda$ ratio falls within the error bars of the experimental point. It is remarkable that the large difference between the t/p and ${}^3_\Lambda\mathrm{H}/\Lambda$ ratios is reproduced without any additional parameters. Rapidity distributions of ${}^3_\Lambda\mathrm{H}/\Lambda$ and ${}^4_\Lambda\mathrm{He}/\Lambda$ ratios are predicted. Midrapidity mean transverse momenta of protons, Λ's and light (hyper)nuclei in central collisions agree well with the data. The calculated directed flow also reasonably well reproduces of the data.

DOI: 10.1103/PhysRevC.109.034901

I. INTRODUCTION

Hypernuclei are an important topic of nuclear physics. Heavy-ion reactions at relativistic energies are an abundant source of strangeness and are therefore well suited for the production of light hypernuclei. The interest in studying hypernuclei in collisions of heavy ions is twofold. First, heavy-ion experiments give us information on lifetimes and binding energies of light hypernuclei; see, e.g., [1–4]. This allow us to refine out understanding of hyperon-nucleon interactions and the role of flavor symmetry that are relevant for nuclear structure [5–7] and astrophysics [8–10], as well as for construction of the hadronic equation of state (EoS) for applications to heavy-ion collisions [11]. Another aspect of studying production of hypernuclei is directly related to diagnostics of the quark-gluon plasma (QGP) formation in heavy-ion collisions. It was suggested that the strangeness population factor $S_3 = ({}^3_\Lambda\mathrm{H}/{}^3\mathrm{He})p/\Lambda$ can serve as a probe of the baryon number and strangeness correlation in the produced matter because of its different behaviors in the QGP and hadronic matter [12–14].

In this paper we focus on discussing the mechanism of hypernuclei formation in heavy-ion collisions. Similarly to the light-nuclei production, alternative mechanisms [13,15–19] are still actively debated. The coalescence [12,13,17,18] and the thermodynamic models [13,18–24] are two of the most popular alternative approaches. The model of parton-hadron quantum molecular dynamics (PHQMD) [15,16] is based on specific procedures of recognition of light (hyper)nuclei. Light (hyper)nuclei in this model are not dynamic objects, but rather are associated with relatively stable clusterlike correlations. Therefore, this approach can be viewed as kinetics of propagation of the correlations. The light nuclei act as dynamic objects in kinetic models of Refs. [25–27] (only deuterons) and [28] (all light nuclei up to ^{4}He). However, these dynamical treatments have not been extended to hypernuclei so far.

As found in Refs. [13,18], both the coalescence and thermodynamic models agree in their predictions for the yields of the light (hyper)nuclei. The thermodynamical approach has an important advantage. It does not need additional parameters for the light-(hyper)nuclei treatment. It describes the light nuclei on an equal basis with hadrons, i.e., in terms of temperatures and chemical potentials. Therefore, its predictive power is the same for light nuclei and hadrons. This approach was first realized within the statistical model [20]. The statistical model gave a good description of even hypernuclei and antinuclei [21].

Recently data on light-hypernuclei production in Au+Au collisions at $\sqrt{s_{NN}} = 3$ GeV appeared [3,29–31], some of them [29,30] preliminary. These data were analyzed in Refs. [16,18,19]. Simulations were performed within the PHQMD approach [16], ultrarelativistic quantum molecular dynamics (UrQMD) + coalescence and UrQMD-hybrid + coalescence approaches were applied in Ref. [18], and the JAM + coalescence model (jet *AA* microscopic transport

*kozhevnikova@jinr.ru

†yivanov@theor.jinr.ru

model [32,33]) was used in STAR papers and presentations [3,29–31]. These data were also analyzed within the hybrid dynamical-statistical approach [19], which is a modification of the statistical multifragmentation model [34].

In the present paper, we extend the light-nuclei treatment of our previous papers [22–24] to hypernuclei production at $\sqrt{s_{NN}} = 3$ GeV. This treatment is based on the updated three-fluid hydrodynamics-based event simulator extended by UrQMD final state interactions (THESEUS) generator [22], in which the light (hyper)nuclei production is considered within the thermodynamic treatment. Our approach is similar to the thermal production from the UrQMD hybrid model in Ref. [13]. We calculate some bulk properties and directed flow of protons, Λ's, and light (hyper)nuclei and compare them with available STAR data. Since the aforementioned coalescence approaches provide a quite reasonable description of the bulk properties, we address the question whether a similar description can be achieved by less demanding means, i.e., using thermodynamics.

II. THE THESEUS GENERATOR

The THESEUS event generator [35,36] is based on the model of the three-fluid dynamics (3FD) [37,38] complemented by the UrQMD [39] for the afterburner stage. The output of the 3FD model consists of fields of local flow velocities and thermodynamic quantities defined on the freeze-out hypersurface. The THESEUS generator transforms the 3FD output into a set of observed particles, i.e., it performs the particlization. The particlization is followed by the UrQMD afterburning stage.

The initial version of THESEUS [35,36] produced the primordial nucleons and hyperons, i.e., both observable nucleons and those bound in the light (hyper)nuclei. These nucleons and hyperons were intended for the subsequent use in the coalescence model, just as was done for the light-nuclei production in Refs. [38,40]. After the coalescence, the nucleons and hyperons bound in the light (hyper)nuclei should be subtracted from the primordial ones. If both nucleons/hyperons and light (hyper)nuclei are sampled from the 3FD output, i.e., temperature and chemical potential fields obtained from the EoS, in which the light (hyper)nuclei are not included, the bound nucleons/hyperons become double counted. This leads to an overestimation of the total baryon charge in the final state containing both baryons and clusters. To avoid this double counting in the updated version of THESEUS [22], the baryon chemical potentials are recalculated proceeding from the local baryon number conservation in the system of hadrons extended by the light-(hyper)nuclei species listed in Table I. The list of the light (hyper)nuclei includes stable nuclei [deuterons (d), tritons (t), helium isotopes ^{3}He and ^{4}He], and low-lying ^{4}He resonances decaying into stable species [41]. As compared to our previous papers [22–24], here we additionally include the stable (with respect to strong decays) hypernuclei $^3_\Lambda$H and $^4_\Lambda$He. The anti(hyper)nuclei are also included.

The light (hyper)nuclei are included on an equal basis with other hadrons in the updated THESEUS [22]. They are sampled similarly to other hadrons. However, there is an important difference between treatments of light (hyper)nuclei and other hadrons. While the hadrons pass through the UrQMD afterburner stage after the particlization, the light (hyper)nuclei do not, because UrQMD is not able to treat them. To partially overcome this shortcoming we imitate the afterburner for light (hyper)nuclei by late freeze-out in the 3FD, following the recipe of Ref. [22].

TABLE I. Stable light (hyper)nuclei and low-lying resonances of the ^{4}He system (from BNL properties of nuclides [42]). J denotes the total angular momentum. The last column represents branching ratios of the decay channels, in percent. The p, n, d correspond to the emission of protons, neutrons, or deuterons, respectively. The hypernuclei are replicated from Refs. [13,43].

Nucleus(E) (MeV)	J	Decay modes (%)
d	1	Stable
t	1/2	Stable
^{3}He	1/2	Stable
^{4}He	0	Stable
^{4}He(20.21)	0	$p = 100$
^{4}He(21.01)	0	$n = 24$, $p = 76$
^{4}He(21.84)	2	$n = 37$, $p = 63$
^{4}He(23.33)	2	$n = 47$, $p = 53$
^{4}He(23.64)	1	$n = 45$, $p = 55$
^{4}He(24.25)	1	$n = 47$, $p = 50$, $d = 3$
^{4}He(25.28)	0	$n = 48$, $p = 52$
^{4}He(25.95)	1	$n = 48$, $p = 52$
^{4}He(27.42)	2	$n = 3$, $p = 3$, $d = 94$
^{4}He(28.31)	1	$n = 47$, $p = 48$, $d = 5$
^{4}He(28.37)	1	$n = 2$, $p = 2$, $d = 96$
^{4}He(28.39)	2	$n = 0.2$, $p = 0.2$, $d = 99.6$
^{4}He(28.64)	0	$d = 100$
^{4}He(28.67)	2	$d = 100$
^{4}He(29.89)	2	$n = 0.4$, $p = 0.4$, $d = 99.2$
$^3_\Lambda$H	1/2	Stable
$^4_\Lambda$He	0	Stable

The calculation of hypernuclei production is the same as that of light nuclei in Ref. [24]. In Ref. [24] it was found that the late freeze-out, characterized by the freeze-out energy density $\varepsilon_{\rm frz} = 0.2$ GeV/fm^3, is preferable for deuterons, tritons, and ^{3}He. We use precisely the same freeze-out for the calculation of the $^3_\Lambda$H production. It was also found [24] that the ^{4}He observables are better reproduced with the standard 3FD freeze-out, $\varepsilon_{\rm frz} = 0.4$ GeV/fm^3, which indicates that the ^{4}He nuclei survive better in the afterburner stage as more spatially compact and tightly bound objects. We use this standard 3FD freeze-out for simulations of the $^4_\Lambda$He production. However, the binding energy of $^4_\Lambda$He ($B_\Lambda \simeq 2.4$ MeV [4]) is similar to that of ^{3}He ($B_N = 2.6$ MeV), which may imply that the late freeze-out is more suitable for the $^4_\Lambda$He production. Therefore, the calculations with the late freeze-out are also presented for $^4_\Lambda$He. Details of the freeze-out procedure in 3FD are described in Refs. [44,45]. Similarly to Ref. [24] three different equations of state (EoS's) are used in the simulations: a purely hadronic EoS [46] (hadr. EoS) and two EoS's with deconfinement [47], i.e., an EoS with a first-order phase transition (1PT EoS) and one with a smooth crossover transition (crossover EoS).

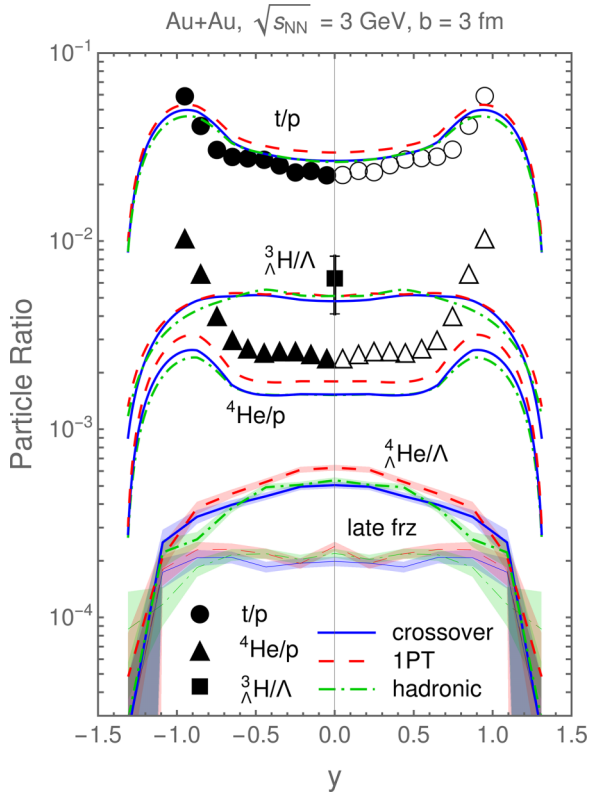

FIG. 1. Rapidity distributions of ratios t/p, ^{4}He$/p$, $^3_\Lambda$H$/\Lambda$, and $^4_\Lambda$He$/\Lambda$ in central ($b = 3$ fm) Au+Au collisions at collision energy of $\sqrt{s_{NN}} = 3$ GeV. Results are calculated with hadronic, 1PT, and crossover EoS's. The t and $^3_\Lambda$H yields are calculated with the late freeze-out, while ^{4}He and $^4_\Lambda$He ones are calculated with the conventional 3FD freeze-out (bold lines). Results for $^4_\Lambda$He with the late freeze-out are also displayed (thin lines marked as "late frz"). Protons and Λs are calculated with the conventional 3FD freeze-out and the subsequent UrQMD afterburner. STAR data for protons and light nuclei (centrality 0–10%) are from Ref. [48]. The $^3_\Lambda$H$/\Lambda$ midrapidity point is taken from Ref. [30]. Full symbols display measured experimental points, whereas the open ones are those reflected with respect to the midrapidity.

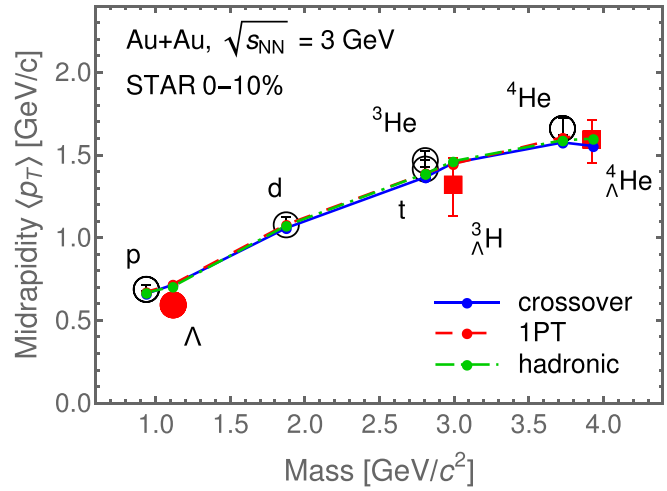

FIG. 2. Midrapidity mean transverse momentum of protons, Λ hyperons, and light (hyper)nuclei in central ($b = 3$ fm) Au+Au collisions at collision energy of $\sqrt{s_{NN}} = 3$ GeV. Results are calculated with hadronic, 1PT, and crossover EoS's. Protons are calculated within the conventional 3FD freeze-out with the subsequent UrQMD afterburner. Deuterons, tritons, ^{3}He, and $^3_\Lambda$H$/\Lambda$ are calculated with the late freeze-out, while ^{4}He and $^4_\Lambda$He are calculated with the conventional 3FD freeze-out. STAR data are from Refs. [29,48].

III. BULK OBSERVABLES

Rapidity distributions of ratios t/p, ^{4}He$/p$, $^3_\Lambda$H$/\Lambda$, and $^4_\Lambda$He$/\Lambda$ in central ($b = 3$ fm) Au+Au collisions at collision energy of $\sqrt{s_{NN}} = 3$ GeV are presented in Fig. 1. The proton and Λ distributions are calculated within full THESEUS, i.e., with the standard 3FD freeze-out and the UrQMD afterburner. The t and $^3_\Lambda$H yields are calculated with the late freeze-out ($\varepsilon_{\rm frz} = 0.2$ GeV/fm^3), while ^{4}He and $^4_\Lambda$He ones are calculated with the conventional 3FD freeze-out ($\varepsilon_{\rm frz} = 0.4$ GeV/fm^3) without the subsequent afterburner. Since the binding energy of $^4_\Lambda$He is similar to that of ^{3}He, we also present calculations for $^4_\Lambda$He production with the late freeze-out. Statistical errors of the $^4_\Lambda$He calculations are displayed by the respective bands.

The strange particles are rare probes at this collision energy. The canonical ensemble with exact strangeness conservation is needed for their description. The calculated yields of Λ's, $^3_\Lambda$H, and $^4_\Lambda$He are considerably overestimated because of grand canonical ensemble used in 3FD. Therefore, we do not demonstrate the Λ, $^3_\Lambda$H, and $^4_\Lambda$He yields by themselves. This grand-canonical overestimation is canceled in the $^3_\Lambda$H$/\Lambda$ and $^4_\Lambda$He$/\Lambda$ ratios.

As seen from Fig. 1, the calculation reasonably well reproduces the nonstrange ratios. The slight overestimation of the t/p ratio is because of underestimation of the proton yield; see Ref. [24]. The ^{4}He is underestimated in our calculations. Apparently, inclusion of light-nuclei resonances with $A = 5$ into the scheme, i.e., those of ^{5}H, ^{5}He, and ^{5}Li [49] that decay into ^{4}He, may correct this underestimation. The calculated result for the midrapidity $^3_\Lambda$H$/\Lambda$ ratio falls within the error bars of the experimental point [30]. It is remarkable that the large difference between the t/p and $^3_\Lambda$H$/\Lambda$ ratios is reproduced without any additional parameters.

The collision process develops in the hadronic phase in all considered scenarios, i.e., hadronic, 1PT and crossover ones. The corresponding EoS's are very similar in the hadronic phase but not identical. Therefore, EoS-induced differences in the ratios indicate uncertainties of the model predictions.

Midrapidity mean transverse momentum of protons, Λ's, and light (hyper)nuclei in central ($b = 3$ fm) collisions is displayed in Fig. 2. This quantity characterizes the radial flow. Curves in Fig. 2 are displayed only for eye guidance. One can see that these curves (for three different EoS's) in fact coincide. Results of the calculations are shown by dots on these curves. Moreover, results for strange and nonstrange species lie on the same curves. The calculated points agree well with the data [29,48]. Even slight deviation of these curves from straight lines is reproduced.

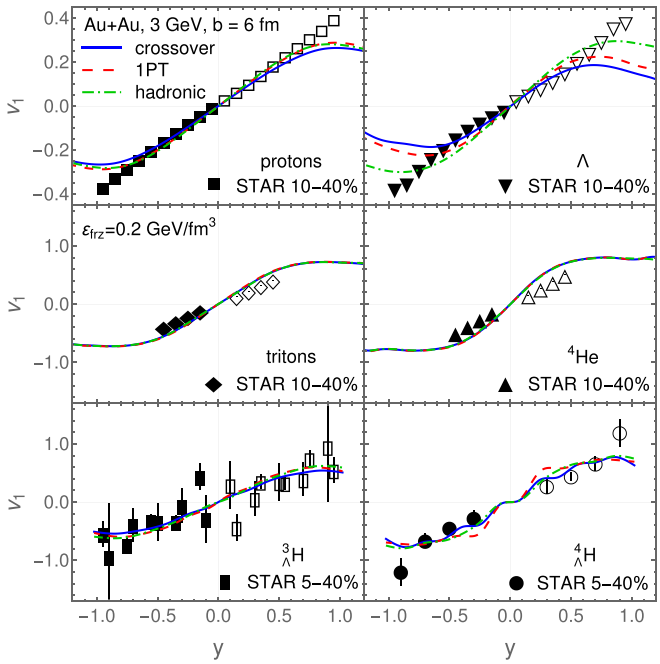

FIG. 3. Directed flow of protons, Λ hyperons, and light (hyper)nuclei (tritons, ^{4}He, $^3_\Lambda$H, and $^4_\Lambda$He) as function of rapidity in semicentral ($b = 6$ fm) Au+Au collisions at collision energy of $\sqrt{s_{NN}} = 3$ GeV. Results are calculated with hadronic, 1PT, and crossover EoS's. The THESEUS simulations for light (hyper)nuclei were performed with the late freeze-out ($\varepsilon_{\rm frz} = 0.2$ GeV/fm^3). The flow of protons and Λ's is calculated with the conventional 3FD freeze-out followed by the subsequent UrQMD afterburner. STAR data are from Refs. [31,50,51]. Full symbols display measured experimental points, whereas the open ones are those reflected with respect to the midrapidity.

IV. DIRECTED FLOW

The directed flow is a more delicate observable. The calculated directed flow of protons, Λ hyperons, and light (hyper)nuclei (tritons, ^{4}He, $^3_\Lambda$H, and $^4_\Lambda$He) as a function of rapidity in semicentral ($b = 6$ fm) Au+Au collisions at collision energy of $\sqrt{s_{NN}} = 3$ GeV is presented in Fig. 3. The results are compared with STAR data [31,50,51]. We do not display results for light nuclei (deuterons and ^{3}He) because they are not directly related to the considered hypernuclei. Results for all light nuclei can be found in Ref. [24]. The THESEUS simulations for light (hyper)nuclei are performed for the late freeze-out ($\varepsilon_{\rm frz} = 0.2$ GeV/fm^3) for three EoS's. The flow of protons and Λ hyperons is calculated within the full THESEUS, i.e., with the conventional 3FD freeze-out and the subsequent UrQMD afterburner.

The directed proton flow is almost independent of the EoS used [24]. The calculated results perfectly (except for very forward and backward rapidities) reproduce the experimental proton flow [51]. Agreement with the data [50] becomes worse with increasing atomic number of the light nucleus. If the calculated midrapidity slope of the triton directed flow is only slightly steeper than the experimental one, for ^{4}He it is already noticeably steeper.

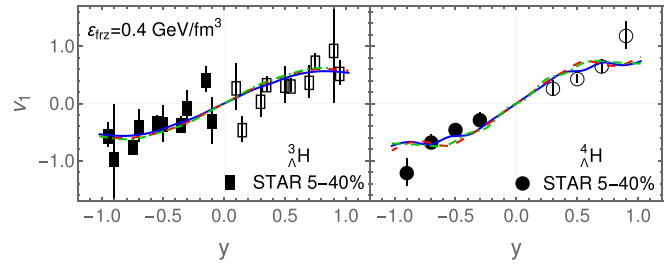

FIG. 4. The same as in Fig. 3 but only for light hypernuclei ($^3_\Lambda$H and $^4_\Lambda$He) calculated with the conventional 3FD freeze-out ($\varepsilon_{\rm frz} = 0.4$ GeV/fm^3).

The directed Λ flow depends on the EoS, while that of hypernuclei is again EoS independent (up to the statistical fluctuations). Apparently the nucleon content of the hypernuclei dominates in the v_1 formation. The crossover scenario results in the best in reproduction of the midrapidity slope of the Λ flow. The $^4_\Lambda$He flow is reproduced to the same extent as that of light nuclei. It is difficult to judge the degree of agreement with the $^3_\Lambda$H flow data because of their large error bars.

In Fig. 3, the directed flow of ^{4}He and $^4_\Lambda$He is calculated with the late freeze-out ($\varepsilon_{\rm frz} = 0.2$ GeV/fm^3) instead of the conventional 3FD freeze-out that is preferable for ^{4}He and presumably for $^4_\Lambda$He. The reason is that the ^{4}He directed flow is independent of the type (late or conventional) of the freeze-out used, as demonstrated in Ref. [24]. Nevertheless, we additionally checked this independence for $^4_\Lambda$He. The results of calculation of v_1 of $^3_\Lambda$H and $^4_\Lambda$He with the conventional 3FD freeze-out is presented in Fig. 4. One can see that the v_1 flows with the conventional freeze-out for both hypernuclei are identical (up to statistical fluctuations) to the late-freeze-out ones. The midrapidity slope of the proton flow also remains unchanged after the afterburner [24]. All this indicates that the baryon directed flow is formed at the early stage of the reaction.

V. SUMMARY

Simulations of the Λ-hyperon and light-hypernuclei production in Au+Au collisions at $\sqrt{s_{NN}} = 3$ GeV were performed within the updated THESEUS event generator [22]. In the updated THESEUS, the light (hyper)nuclei are treated thermodynamically, i.e., they are considered on the equal basis with hadrons. The only additional parameter associated with the light (hyper)nuclei is related to the late freeze-out that imitates the afterburner stage because UrQMD is not able to dynamically treat the light (hyper)nuclei. This is a less demanding way to describe the light-(hyper)nuclei production as compared to the coalescence.

The calculation of hypernuclei production is the same as that of light nuclei in Ref. [24]. In Ref. [24] it was found that the late freeze-out is preferable for deuterons, tritons, and ^{3}He. We used precisely the same freeze-out for the calculation of the $^3_\Lambda$H production. It was also found [24] that the ^{4}He observables are better reproduced with the standard 3FD freeze-out, which indicates that the ^{4}He nuclei survive

better in the afterburner stage as more spatially compact and tightly bound objects. We used this standard 3FD freeze-out for simulations of the ${}^{4}_{\Lambda}$He production. However, the binding energy of ${}^{4}_{\Lambda}$He ($B_\Lambda \simeq 2.4$ MeV [4]) is similar to that of ^{3}He ($B_N = 2.6$ MeV), which may imply that the late freeze-out is more suitable for the ${}^{4}_{\Lambda}$He production. The hypernuclei results were compared with recent STAR data [29–31], as well as with the results of light-nuclei calculations [24].

It is found that the calculated midrapidity ${}^{3}_{\Lambda}\mathrm{H}/\Lambda$ ratio falls within the error bars of the experimental point [30]. It is remarkable that the large difference between the t/p and ${}^{3}_{\Lambda}\mathrm{H}/\Lambda$ ratios is reproduced without any additional parameters. Rapidity distributions of ${}^{3}_{\Lambda}\mathrm{H}/\Lambda$ and ${}^{4}_{\Lambda}\mathrm{He}/\Lambda$ ratios are predicted. Midrapidity mean transverse momenta of protons, Λ's and light (hyper)nuclei in central collisions agree well with the data [29,30]. The calculated directed flow also reasonably well reproduces the data [31]. The directed flow turned out to be independent of the type (late or conventional) of the freeze-out. This indicates that the baryon directed flow is formed at the early stage of the reaction.

ACKNOWLEDGMENTS

We are sincerely grateful to Iurii Karpenko and David Blaschke who made enormous contributions in the early stage of this project. Fruitful discussions with D. N. Voskresensky are gratefully acknowledged. This work was carried out using computing resources of the federal collective usage center "Complex for simulation and data processing for mega-science facilities" at NRC "Kurchatov Institute" [52] and computing resources of the supercomputer "Govorun" at JINR [53].

[1] L. Adamczyk *et al.* (STAR Collaboration), Measurement of the ${}^{3}_{\Lambda}\mathrm{H}$ lifetime in Au+Au collisions at the BNL Relativistic Heavy Ion Collider, Phys. Rev. C **97**, 054909 (2018).

[2] S. Acharya *et al.* (ALICE Collaboration), ${}^{3}_{\Lambda}\mathrm{H}$ and ${}^{3}_{\bar{\Lambda}}\overline{\mathrm{H}}$ lifetime measurement in Pb-Pb collisions at $\sqrt{s_{\mathrm{NN}}} = 5.02$ TeV via two-body decay, Phys. Lett. B **797**, 134905 (2019).

[3] M. Abdallah *et al.* (STAR Collaboration), Measurements of ${}^{3}_{\Lambda}\mathrm{H}$ and ${}^{4}_{\Lambda}\mathrm{H}$ lifetimes and yields in Au+Au collisions in the high baryon density region, Phys. Rev. Lett. **128**, 202301 (2022).

[4] M. Abdallah *et al.* (STAR Collaboration), Measurement of ${}^{4}_{\Lambda}\mathrm{H}$ and ${}^{4}_{\Lambda}\mathrm{He}$ binding energy in Au+Au collisions at $\sqrt{s_{NN}} =$ 3 GeV, Phys. Lett. B **834**, 137449 (2022).

[5] A. Gal, E. V. Hungerford, and D. J. Millener, Strangeness in nuclear physics, Rev. Mod. Phys. **88**, 035004 (2016).

[6] M. Knöll and R. Roth, Hyperon-nucleon interaction constrained by light hypernuclei, Phys. Lett. B **846**, 138258 (2023).

[7] H. Le, J. Haidenbauer, U.-G. Meißner, and A. Nogga, Separation energies of light Λ hypernuclei and their theoretical uncertainties, Eur. Phys. J. A **60**, 3 (2024).

[8] D. Lonardoni, A. Lovato, S. Gandolfi, and F. Pederiva, Hyperon puzzle: Hints from quantum Monte Carlo calculations, Phys. Rev. Lett. **114**, 092301 (2015).

[9] K. A. Maslov, E. E. Kolomeitsev, and D. N. Voskresensky, Solution of the hyperon puzzle within a relativistic mean-field model, Phys. Lett. B **748**, 369 (2015); Making a soft relativistic mean-field equation of state stiffer at high density, Phys. Rev. C **92**, 052801(R) (2015); Relativistic mean-field models with scaled hadron masses and couplings: Hyperons and maximum neutron star mass, Nucl. Phys. A **950**, 64 (2016).

[10] M. Fortin, S. S. Avancini, C. Providência, and I. Vidaña, Hypernuclei and massive neutron stars, Phys. Rev. C **95**, 065803 (2017).

[11] A. S. Khvorostukhin, V. D. Toneev, and D. N. Voskresensky, Equation of state for hot and dense matter: σ-ω-ρ model with scaled hadron masses and couplings, Nucl. Phys. A **791**, 180 (2007); Relativistic mean-field model with scaled hadron masses and couplings, *ibid.* **813**, 313 (2008).

[12] S. Zhang, J. H. Chen, H. Crawford, D. Keane, Y. G. Ma, and Z. B. Xu, Searching for onset of deconfinement via hypernuclei and baryon-strangeness correlations, Phys. Lett. B **684**, 224 (2010).

[13] J. Steinheimer, K. Gudima, A. Botvina, I. Mishustin, M. Bleicher, and H. Stocker, Hypernuclei, dibaryon and antinuclei production in high energy heavy ion collisions: Thermal production versus coalescence, Phys. Lett. B **714**, 85 (2012).

[14] T. Shao, J. Chen, C. M. Ko, K. J. Sun, and Z. Xu, Yield ratio of hypertriton to light nuclei in heavy-ion collisions from $\sqrt{s_{\mathrm{NN}}} =$ 4.9 GeV to 2.76 TeV, Chin. Phys. C **44**, 114001 (2020).

[15] J. Aichelin, E. Bratkovskaya, A. Le Fèvre, V. Kireyeu, V. Kolesnikov, Y. Leifels, V. Voronyuk, and G. Coci, Parton-hadron-quantum-molecular dynamics: A novel microscopic n-body transport approach for heavy-ion collisions, dynamical cluster formation, and hypernuclei production, Phys. Rev. C **101**, 044905 (2020).

[16] S. Gläßel, V. Kireyeu, V. Voronyuk, J. Aichelin, C. Blume, E. Bratkovskaya, G. Coci, V. Kolesnikov, and M. Winn, Cluster and hypercluster production in relativistic heavy-ion collisions within the parton-hadron-quantum-molecular-dynamics approach, Phys. Rev. C **105**, 014908 (2022).

[17] Z. Q. Feng, Dynamics of light hypernuclei in collisions of ^{197}Au+^{197}Au at GeV energies, Eur. Phys. J. A **57**, 18 (2021).

[18] T. Reichert, J. Steinheimer, V. Vovchenko, B. Dönigus, and M. Bleicher, Energy dependence of light hypernuclei production in heavy-ion collisions from a coalescence and statistical-thermal model perspective, Phys. Rev. C **107**, 014912 (2023).

[19] N. Buyukcizmeci, T. Reichert, A. S. Botvina, and M. Bleicher, Nucleosynthesis of light nuclei and hypernuclei in central Au+Au collisions at $\sqrt{s_{NN}} = 3$ GeV, Phys. Rev. C **108**, 054904 (2023).

[20] A. Andronic, P. Braun-Munzinger, J. Stachel, and H. Stocker, Production of light nuclei, hypernuclei and their antiparticles in relativistic nuclear collisions, Phys. Lett. B **697**, 203 (2011).

[21] A. Andronic, P. Braun-Munzinger, K. Redlich, and J. Stachel, Decoding the phase structure of QCD via particle production at high energy, Nature (London) **561**, 321 (2018).

[22] M. Kozhevnikova, Y. B. Ivanov, I. Karpenko, D. Blaschke, and O. Rogachevsky, Update of the three-fluid hydrodynamics-based event simulator: Light-nuclei production in heavy-ion collisions, Phys. Rev. C **103**, 044905 (2021).

[23] M. Kozhevnikova and Y. B. Ivanov, Light-nuclei production in heavy-ion collisions within a thermodynamical approach, Phys. Rev. C **107**, 024903 (2023); M. Kozhevnikova and Y.B. Ivanov,

Light-nuclei production in heavy-ion collisions at $\sqrt{s_{NN}} =$ 6.4–19.6 GeV in THESEUS generator based on three-fluid dynamics, Particles **6**, 440 (2023).

[24] M. Kozhevnikova and Yu. B. Ivanov, Light-nuclei production in Au+Au collisions at $\sqrt{s_{NN}} = 3$ GeV within a thermodynamical approach: Bulk properties and collective flow, Phys. Rev. C **109**, 014913 (2024).

[25] D. Oliinychenko, L. G. Pang, H. Elfner, and V. Koch, Microscopic study of deuteron production in PbPb collisions at $\sqrt{s} = 2.76$ TeV via hydrodynamics and a hadronic afterburner, Phys. Rev. C **99**, 044907 (2019).

[26] J. Staudenmaier, D. Oliinychenko, J. M. Torres-Rincon, and H. Elfner, Deuteron production in relativistic heavy ion collisions via stochastic multiparticle reactions, Phys. Rev. C **104**, 034908 (2021).

[27] K. J. Sun, R. Wang, C. M. Ko, Y. G. Ma, and C. Shen, Relativistic kinetic approach to light nuclei production in high-energy nuclear collisions, arXiv:2106.12742.

[28] K. J. Sun, R. Wang, C. M. Ko, Y. G. Ma, and C. Shen, Unveiling the dynamics of little-bang nucleosynthesis, Nature Commun. **15**, 1074 (2024).

[29] Y. Ji *et al.* (STAR Collaboration), Measurements on the production and properties of light hypernuclei at STAR, EPJ Web Conf. **276**, 04003 (2023).

[30] Y. Ji, talk at Quark Matter, https://indico.cern.ch/event/1139644/contributions/5456392/attachments/2707583/4708403/talk_FXT_H3L_Sep08_v11.pdf (2023).

[31] B. Aboona *et al.* (STAR Collaboration), Observation of directed flow of hypernuclei ${}^{3}_{\Lambda}\mathrm{H}$ and ${}^{4}_{\Lambda}\mathrm{H}$ in $\sqrt{s_{NN}} = 3$ GeV Au+Au collisions at RHIC, Phys. Rev. Lett. **130**, 212301 (2023).

[32] Y. Nara, N. Otuka, A. Ohnishi, K. Niita, and S. Chiba, Relativistic nuclear collisions at 10*A* GeV energies from $p +$ Be to Au+Au with the hadronic cascade model, Phys. Rev. C **61**, 024901 (1999).

[33] M. Isse, A. Ohnishi, N. Otuka, P. K. Sahu, and Y. Nara, Mean-field effects on collective flow in high-energy heavy-ion collisions at 2–158*A* GeV energies, Phys. Rev. C **72**, 064908 (2005).

[34] J. P. Bondorf, A. S. Botvina, A. S. Ilinov, I. N. Mishustin, and K. Sneppen, Statistical multifragmentation of nuclei, Phys. Rep. **257**, 133 (1995).

[35] P. Batyuk, D. Blaschke, M. Bleicher, Y. B. Ivanov, I. Karpenko, S. Merts, M. Nahrgang, H. Petersen, and O. Rogachevsky, Event simulation based on three-fluid hydrodynamics for collisions at energies available at the Dubna Nuclotron-based Ion Collider Facility and at the Facility for Antiproton and Ion Research in Darmstadt, Phys. Rev. C **94**, 044917 (2016).

[36] P. Batyuk, D. Blaschke, M. Bleicher, Y. B. Ivanov, I. Karpenko, L. Malinina, S. Merts, M. Nahrgang, H. Petersen, and O. Rogachevsky, Three-fluid hydrodynamics-based event simulator extended by UrQMD final state interactions (THESEUS) for FAIR-NICA-SPSBES/RHIC energies, EPJ Web Conf. **182**, 02056 (2018).

[37] Y. B. Ivanov, Alternative scenarios of relativistic heavy-ion collisions: I. Baryon stopping, Phys. Rev. C **87**, 064904 (2013).

[38] Y. B. Ivanov, V. N. Russkikh, and V. D. Toneev, Relativistic heavy-ion collisions within three-fluid hydrodynamics: Hadronic scenario, Phys. Rev. C **73**, 044904 (2006).

[39] S. A. Bass, M. Belkacem, M. Bleicher, M. Brandstetter, L. Bravina, C. Ernst, L. Gerland, M. Hofmann, S. Hofmann, J. Konopka *et al.*, Microscopic models for ultrarelativistic heavy ion collisions, Prog. Part. Nucl. Phys. **41**, 255 (1998).

[40] Y. B. Ivanov and A. A. Soldatov, Light fragment production at CERN Super Proton Synchrotron, Eur. Phys. J. A **53**, 218 (2017).

[41] E. Shuryak and J. M. Torres-Rincon, Baryon preclustering at the freeze-out of heavy-ion collisions and light-nuclei production, Phys. Rev. C **101**, 034914 (2020).

[42] https://www.nndc.bnl.gov/nudat3/getdataset.jsp?nucleus=4HE&unc=nds.

[43] D. H. Davis, 50 years of hypernuclear physics. I. The early experiments, Nucl. Phys. A **754**, 3 (2005).

[44] V. N. Russkikh and Yu. B. Ivanov, Dynamical freeze-out in trhee-fluid hydrodynamics, Phys. Rev. C **76**, 054907 (2007).

[45] Yu. B. Ivanov and V. N. Russkikh, On freeze-out problem in relativistic hydrodynamics, Phys. At. Nucl. **72**, 1238 (2009).

[46] I. N. Mishustin, V. N. Russkikh, and L. M. Satarov, Fluid dynamical model of relativistic heavy ion collision, Sov. J. Nucl. Phys. **54**, 260 (1991).

[47] A. S. Khvorostukin, V. V. Skokov, V. D. Toneev, and K. Redlich, Lattice QCD constraints on the nuclear equation of state, Eur. Phys. J. C **48**, 531 (2006).

[48] STAR Collaboration, Production of protons and light nuclei in Au+Au collisions at $\sqrt{s_{\mathrm{NN}}} = 3$ GeV with the STAR detector, arXiv:2311.11020.

[49] V. Vovchenko, B. Dönigus, B. Kardan, M. Lorenz, and H. Stoecker, Feeddown contributions from unstable nuclei in relativistic heavy-ion collisions, Phys. Lett. B **809**, 135746 (2020).

[50] M. S. Abdallah *et al.* (STAR Collaboration), Light nuclei collectivity from $\sqrt{s_{NN}} = 3$ GeV Au+Au collisions at RHIC, Phys. Lett. B **827**, 136941 (2022).

[51] M. S. Abdallah *et al.* (STAR Collaboration), Disappearance of partonic collectivity in $\sqrt{s_{NN}} = 3$ GeV Au+Au collisions at RHIC, Phys. Lett. B **827**, 137003 (2022).

[52] http://ckp.nrcki.ru/.

[53] http://hlit.jinr.ru/supercomputer_govorun/.